Dynamic Model for Thrust Generation of Marine Propellers

Blanke, Mogens; Lindegaard, Karl-Petter; Fossen, Thor I.

Published in:
Manoeuvring and control of marine craft 2000 (MCMC 2000)

Publication date:
2000

Document Version
Publisher's PDF, also known as Version of record

DYNAMIC MODEL FOR THRUST GENERATION OF MARINE PROPELLERS

Mogens Blanke [*] **Karl-Petter Lindegaard** [**]
Thor I. Fossen [**]

[*] *Department of Automation, Technical University of Denmark, DK-2800 Kgs. Lyngby, Denmark*
[**] *Department of Engineering Cybernetics, Norwegian University of Science and Technology, N-7491 Norway*

Abstract: Mathematical models of propeller thrust and torque are traditionally based on steady state thrust and torque characteristics obtained in model basin or cavitation tunnel tests. Experimental results showed that these quasi steady state models do not accurately describe the transient phenomena in a thruster. A recently published dynamic model was based on the experimental observations. Describing zero advance speed conditions accurately, this model, however, does not work for a vessel at non-zero relative water speed. This paper derives a large signal dynamic model of propeller that includes the effects of transients in the flow over a wide range of operation. The results are essential for accurate thrust control in dynamic positioning and in underwater robotics.

Keywords: propellers, thrusters, dynamic positioning, underwater robotics, thrust control

1. INTRODUCTION

Underwater vehicle (UUV) speed and position control systems are subject to an increased focus with respect to performance and safety. This is due to an increased number of commercially and militarily applications of UUVs. So far most focus has been directed towards the design of the outer-loop control system, that is speed and positioning control systems while the design of the propeller servo loops have received less attention. Fault monitoring and diagnosis are achieving increasing attention as well to enhance safety and reliability of marine vessels. Both areas require more accurate dynamic models. The control system motivation for better dynamic models is that better models give better control performance. The motivation from fault diagnosis is that better models give faster detection of not-normal operation.

When designing a thruster control system, forces and moments are realized by a propeller control system using a mapping from thrust demand to propeller revolution. This is a non-trivial task since a propeller in water suffers several phenomena that cause thrust losses. Similar mapping would be the basis for diagnostic tools that supervise thruster performance.

The main phenomenon to consider is thrust losses caused by axial water inflow, the speed u_p of the water going into the propeller. The axial flow velocity will in general differ from the speed of the vehicle. The dynamics of the propeller axial flow is usually neglected when designing the propeller shaft speed controller. This leads to thrust degradation since the computed thruster force is a function of both the propeller shaft speed and axial flow. The magnitude of the axial flow velocity will strongly influence the thrust at high speed so it is crucial for the propeller performance. In a diagno-

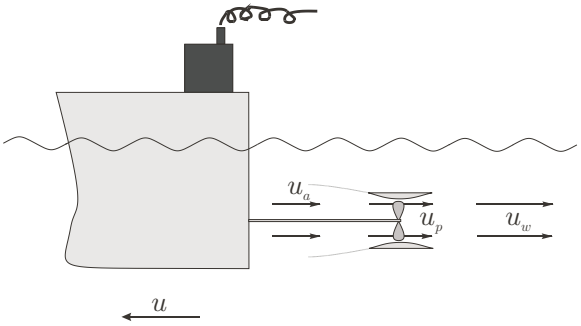

Fig. 1. Definitions of axial flow velocity u_p, advance speed u_a and vehicle speed u.

sis system, incorrect modelling could lead to false alarm for degraded propeller performance caused by transient flow phenomena. Alternatively the diagnosis thresholds would be set so high that real faults would not be diagnosed at an early stage of development. Results from experiments showed that dynamic effects play a significant role which was not accounted for in steady state models.

In (Yoerger *et al.*, 1991) a one-state model for propeller shaft speed n with thrust torque T as output was proposed.

This model can be written:

$$J_m \dot{n} + K_{n|n|} n \, |n| = Q_m \tag{1}$$

$$T = T(n, u_p) \tag{2}$$

where Q_m is the control input (shaft torque). It is convenient to assume that $u_p = 0$ when computing T.

(Healey *et al.*, 1995) modified the models (1)–(2) to describe overshoots in thrust which are typical in experimental data. Based on the results of Cody (Cody, 1992) and McLean (McLean, 1991), Healey and co-workers proposed a *two-state model:*

$$J_m \dot{n} + K_n n = Q_m - Q \tag{3}$$

$$m_f \dot{u}_p + d_f (u_p - u) \, |u_p - u| = T \tag{4}$$

$$T = T(n, u_p) \tag{5}$$

$$Q = Q(n, u_p) \tag{6}$$

Here n is the shaft speed, u_p is the axial flow velocity in the propeller disc and u is the forward speed of the vehicle. This was done by modelling a control volume of water around the propeller as a *mass-damper* system.

Experimental verifications of the one-state and two-state models are found in (Whitcomb and Yoerger, 1999). The model of Healey includes the dynamic flow effects that occur during increase or decrease of the thruster shaft torque and the experimental verification indicates that the model is sound around zero vessel speed. It fails, however, when the vessel speed is nonzero, i.e. makes speed through water or is subject to current.

The problem with nonzero vessel speed relative to water is that the propeller is loaded differently in this condition, and lift and lifting line theories have to be employed to adequately include these phenomena. This paper extends the earlier results to a model that is valid over a range of operation of a marine propellers. The paper starts with looking at the induced axial and tangential velocities in the propeller race, combines this with the classical momentum theory, and assumes a volume of water is accelerated/decelerated in transient conditions. Assessment of propeller thrust is done by employing lifting line theory results and the final propeller model is obtained using lift result on the elements of a propeller blade. Simulation results illustrate the features of the new model. The propeller theory adopted for our purpose is well known (see (Lewis, 1988),(Breslin and Andersen, 1994)), but the combination into a dynamic control model is believed to be a new contribution.

2. NOMENCLATURE

A_p	Propeller disc area (m^2)
u	Surge speed of vehicle (m/s)
u_p	Axial flow velocity in disc (m/s)
u_a	Ambient water velocity (m/s)
n	Propeller shaft speed (rad/s)
X_u	Linear coefficient in surge (kg/s)
$X_{u\|u\|}$	Quadratic coefficient (kg/m)
$X_{\dot{u}}$	Added mass in surge (kg)
t	Thrust deduction number (-)
w	Wake fraction number (-)
m_f	Mass of in control volume (kg)
m	Mass of vehicle (kg)
d_{f0}	Linear damping (kg/s)
d_f	Quadratic damp. (kg/m)
J_m	Inertia for motor/propeller (kgm^2)
Q_m	Motor control torque (Nm)
C_L	Lift coefficient (-)
D	Propeller diameter (m)
T	Propeller thrust (N)
Q	Propeller torque (Nm)
J_0	Advance ratio (-)
K_T	Thrust coefficient (-)
K_Q	Torque coefficient (-)
ρ	Density of water (kg/m^3)
β_i	Angle of attack (rad)
$T_{n\|n\|}$	Thrust coefficient (kgm)
$T_{\|n\|u_a}$	Thrust coefficient (kg)
$Q_{n\|n\|}$	Torque coefficient (kgm^2)
$Q_{\|n\|u_a}$	Torque coefficient (kgm)
$R(u)$	Hull resistance (N)

3. DYNAMIC FLOW

With reference to the notation of Fig. 1, looking at a Bernoulli tube that comprises the propeller, we have Bernoulli's law upstream,

$$p_a + \frac{1}{2}\rho u_a^2 = p_u + \frac{1}{2}\rho u_p^2 \tag{7}$$

and downstream

$$p_a + \frac{1}{2}\rho u_w^2 = p_d + \frac{1}{2}\rho u_p^2 \tag{8}$$

The dynamics of a mass of water in the Bernoulli tube is a quantity m_f as empirical mass

$$m_f \dot{u}_p = T_p + A_p(p_u - p_d) \tag{9}$$

With Eq. 7 less Eq. 8 this is also

$$m_f \dot{u}_p = T_p + \frac{1}{2}\rho A_p(u_a^2 - u_w^2)$$

The usual result from momentum theory (Lewis, 1991) gives

$$u_p = \frac{1}{2}(u_a + u_w) \Longleftrightarrow u_w = 2u_p - u_a \tag{10}$$

Combining Equations 9, 8 and 7 gives

$$m_f \dot{u}_p + \frac{1}{2}\rho A_p(u_w^2 - u_a^2) = T_p$$

insertion of the momentum theory result Eq. 10 yields

$$m_f \dot{u}_p + 2\rho A_p u_p(u_p - u_a) = T_p \tag{11}$$

This equation is only valid for quasi-stationary flow, not for u and u_p having opposite signs simply because we can't use Bernoulli's law on that case. Further, negative speed is not accounted for. Thus we need to write Eq. 11 as

$$m_f \dot{u}_p + 2\rho A_p |u_p| (u_p - u_a) = T_p \tag{12}$$

It remains to find other constraints between values of T_p and u_p since Eq. 12 only gives an implicit relation and T_p obviously will be a function of u_p.

4. BLADE SECTION FORCES

The basic lift theory for a section of a propeller blade is well known indeed, but hydrodynamic literature concentrates on iterative design solutions for the propeller itself in a steady state and does not provide the type of dynamic model of thrust and torque that is needed for control.

This section adopts the basic hydrodynamic theory to formulate a dynamic model using the instantaneous axial flow as one of the states. This model will subsequently be compared with the steady-state hydrodynamic model which is commonly available in the form of the propeller characteristics.

Lift theory applied to a propeller considers a section of a blade at radius R. The chord at this section is c. The relative velocity of the element is

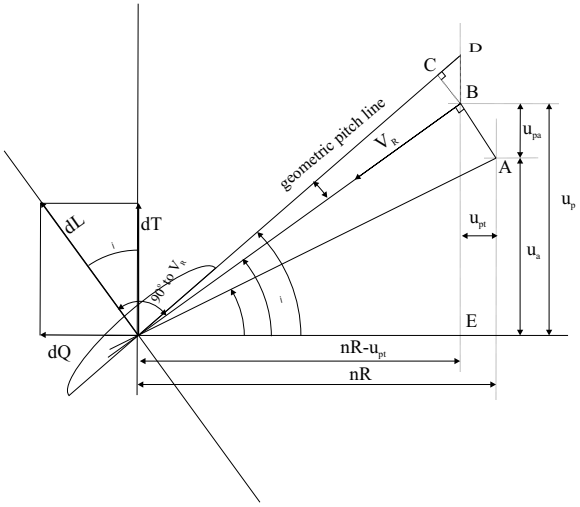

Fig. 2. Flow velocity diagram for a section of a propeller blade with rotational speed n rad/s. u_a is the undisturbed inflow velocity to the screw propeller. u_{pt} and u_{pa} are tangential and axial induced velocities. β_i is the hydrodynamic angle of attack and α the insidence angle to the blade section. The relative velocity V_R and α determine the lift force.

V_R. Lift theory states that the force components on the section are lift and drag. The lift is

$$L = \frac{\rho}{2} c\ dr\ \ |V_R|\, V_R\ C_L(\alpha)$$

where $C_L(\alpha)$ is the lift coefficient of the profile for an angle α of incidence. We start with assuming a non-viscous fluid and expand later to the viscous case.

A velocity diagram for a blade section is shown in Fig. 2 for the non-viscous case. The Figure shows the hydrodynamic pitch angle β_i, the advance angle β and the propellers pitch line θ. The angle of incidence is $\alpha = \theta - \beta_i$. At a radius R of the propeller,

$$\tan\beta = \frac{u_a}{nR}$$

and

$$\tan\beta_i = \frac{u_a + u_{pa}}{nR - u_{pt}}$$

The effective radial velocity is

$$\overleftarrow{OE} = nR - u_{pt}$$

where n is in rad/s. The effective axial speed is $\overrightarrow{EB} = \overrightarrow{u}_p = \overrightarrow{u}_a + \overrightarrow{u}_{pt}$. The open water advance velocity (without propeller) is $\overrightarrow{EA} = \overrightarrow{u}_a$. Inspection of the geometry of the Figure shows that $\overrightarrow{CB} = \overrightarrow{V}_R \sin\alpha$ and $\overrightarrow{BC} \perp \overrightarrow{OD}$. Then, since $\alpha + \beta_i = \theta$, $\overrightarrow{BD}\cos(\theta) = \overrightarrow{CB} = \overrightarrow{V}_R \sin(\alpha)$. Further, elementary manipulation gives $\overrightarrow{ED} = \overrightarrow{u}_p + \overrightarrow{BD} = (\overrightarrow{nR} - \overrightarrow{u}_{pt})\tan(\alpha + \beta_i) \Rightarrow \overrightarrow{V}_R \sin(\alpha) = \overrightarrow{u}_p \cos(\theta) - (\overrightarrow{nR} - \overrightarrow{u}_{pt})\sin(\theta)$.

Lift on an element dr of the blade is, using the usual approximation for lift $C_L(\alpha) = C_L \sin(\alpha)$,

$$dL = \frac{\rho}{2} c dr C_L \left|V_R\right| V_R \sin(\alpha) \tag{13}$$

Drag is similarly

$$dD = \frac{\rho}{2} c dr C_D \left|V_R\right| V_R \sin(\alpha) \tag{14}$$

In a non-viscous fluid, thrust is hence

$$\begin{gathered} dT = dL\cos(\beta_i) = \\ \frac{\rho}{2} c dr C_L \ \left|nR - u_{pt}\right| \ ((u_a + u_{pa})\cos(\theta) \\ -(nR - u_{pt})\sin(\theta)) \end{gathered} \tag{15}$$

and torque amounts to

$$\begin{gathered} dQ = R\ dL\sin(\beta_i) = \\ \frac{\rho}{2} c R dr C_L \ \left|nR - u_{pt}\right| ((u_a + u_{pa})\cos(\theta) \\ -(nR - u_{pt})\sin(\theta)) \end{gathered} \tag{16}$$

We note that the dT and dQ terms are quadratic. We finally note that when there are no friction losses, the power balance for the section of the disc gives

$$dQ(n - \frac{u_{pt}}{R}) = dT\,(u_a + u_{pa}) \tag{17}$$

The ideal efficiency for the blade element is

$$\eta_I = \frac{dT\ u_a}{dQ\ \omega} = \frac{nR - u_{pt}}{u_a + u_{pa}} \frac{u_a}{nR} = \frac{\tan\beta}{\tan\beta_i}$$

We later need the definitions

$$a = \frac{u_{pa}}{u_{pa}},\ a' = \frac{u_{pt}}{nR}$$

then the hydrodynamic angle of attack is related to the geometric angle β as

$$\tan\beta_i = \frac{1+a}{1-a'}\tan\beta \tag{18}$$

5. RELATION TO OPEN WATER PROPELLER DATA

Propeller data are commonly presented in the form of non-dimensional propeller data. A plot of K_q and K_t versus J is shown in Fig. 3

The characteristic is linear over a wide range of advance, and a linear representation in J is valid over this range,

$$\begin{aligned} K_T &= \alpha_0 + \alpha_1 J \\ K_Q &= \beta_0 + \beta_1 J \end{aligned} \tag{19}$$

Using the nondimensionalisation of thrust, torque and advance number, this is equivalent to a quadratic model (Blanke, 1982), (Fossen, 1994),

$$\begin{aligned} T &= T_{n|n|} n|n| - T_{|n|u_a}|n|u_a \\ Q &= Q_{n|n|} n|n| - Q_{|n|u_a}|n|u_a \end{aligned} \tag{20}$$

where

$$\begin{aligned} T_{n|n|} &= \rho D^4 \alpha_0 \quad Q_{n|n|} = \rho D^5 \beta_0 \\ T_{|n|u_a} &= \rho D^3 \alpha_1 \ Q_{|n|u_a} = \rho D^4 \beta_1 \end{aligned} \tag{21}$$

The coefficient $T_{|n|u_a}$ is derived from steady state where u_p has achieved its final value.

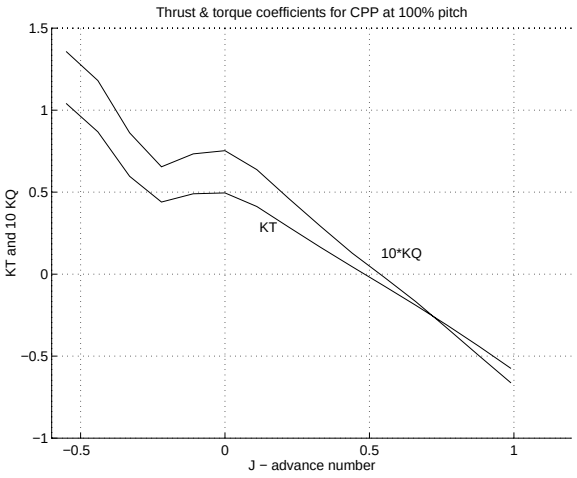

Fig. 3. Non dimensional thrust K_T and torque K_Q versus advance number, here expressed as $J = \frac{2\pi\ u_a}{nD}$. The curves are with 100% pitch angle.

To explicitly account for the dynamic variation in axial water speed, we formulate the revised thrust and torque model as

$$\begin{aligned} T_p(n, u_p) &= T^o_{|n|n}|n|n + T^o_{|n|v}\,|n|\,u_p \\ Q_p(n, u_p) &= Q_{|n|n}|n|n + Q^o_{|n|v}\,|n|\,u_p \end{aligned} \tag{22}$$

where the relation of parameters in the open water characteristics are

$$T^o_{|n|v} = \frac{1}{1+a} T_{|n|v},\ Q^o_{|n|v} = \frac{1}{1+a} Q_{|n|v} \tag{23}$$

Combining Equations (22) with (12) gives the revised model.

Remark 1: Including drag in the model would not be difficult. The thrust equation would then read $dT = dLcos\beta_i - dD\sin\beta_i$ and similar for torque. This equation has the same quadratic form as Eq. 15 but a square term $T_{|u_p|u_p}|u_p|u_p$ would be added. This means the K_T propeller approximation in J would not be linear but include a J^2term. There is no difficulty in adding this term, nor in getting its parameter from the propeller characteristic. Therefore, as long as the accuracy of the linear approximation is satisfactory, we can disregard drag from the propeller blade, otherwise the square term in u_p should be added. The same goes for the torque equation.

6. DYNAMIC LARGE SIGNAL MODEL

For a fixed pitch propeller, the nonlinear state equations have three states, propeller shaft speed, vessel speed relative to water and inflow velocity at the propeller disc.

The acceleration of the shaft is given by the torque balance,

$$J_m \dot{n} = Q_{eng} - Q_{|n|n}|n|n + Q^o_{|n|v}\,|n|\,u_p \tag{24}$$

Acceleration of water at the propeller disc by

$$m_f \dot{u}_p + 2\rho A_p |u_p| (u_p - u_a) \quad (25)$$
$$= T_{|n|n}|n|n + T^o_{|n|v}|n| u_p$$

and Vessel speed is determined from the balance between resistance and effective thrust

$$m_s \dot{u} = R(u) + (1-t)T_p(n, u_p) \quad (26)$$

where the average flow at the propeller disc (when the propeller does not produce thrust) is that of the vessel reduced by the wake fraction

$$u_a = (1-w)u \quad (27)$$

The propeller thrust in transient and steady state condition, at any value of n, u_a and u_p is

$$T_p(n, u_p) = T_{|n|n}|n|n + T^o_{|n|v}|n| u_p \quad (28)$$

The advantage of this model over recently published dynamic propeller models is that this model is valid also when the ship makes speed through water or is subject to current.

Remark 2: Damping in surge is modeled as the sum of *linear laminar skin friction,* $-X_u u$, (see Faltinsen and Sortland (Faltinsen and Sortland, 1987)) and *nonlinear quadratic drag,* $-X_{u|u|}u|u|$ (see Faltinsen (Faltinsen, 1990)).

$$R(u) = -X_u u - X_{u|u|}u|u| \quad (29)$$

Similarly, linear damping, $d_{f0}u_p$, is included in the axial flow model since quadratic damping, $d_f|u_p|u_p$, alone would give an unrealistic response at low speeds (zero quadratic damping at zero speed).

Hence, the axial flow model reads

$$m_f \dot{u}_p + d_{f0}u_p + d_f |u_p| (u_p - u_a) \quad (30)$$
$$= T_{|n|n}|n|n + T^o_{|n|v}|n| u_p \quad (31)$$

Remark 3: Phenomena that were not included in the model were drag effects, cross-coupling drag, varying wake with turn or sway, air suction, and possible interaction between several thrusters and/or the hull.

Remark 4. The dynamics of the tangential flow u_{pt} could play an essential role for the thrust dynamics as well as the axial flow that is the main concern in this paper. The modelling and verification of tangential flow dynamics would be a natural extension of the present model.

6.1 *Parameter Selection*

At steady state, the derivatives are all zero, i.e. $\dot{u} = \dot{u}_p = 0$. Then,

$$-X_u \bar{u} - X_{u|u|}\bar{u}|\bar{u}| = (1-t)T \quad (32)$$
$$d_{f0}\bar{u}_p + d_f|\bar{u}_p|(\bar{u}_p - \bar{u}_a) = T \quad (33)$$

m	1000 $[kg]$	w	0.2
$-X_{\dot{u}}$	$0.05m$ $[kg]$	t	0.1
$-X_u$	0.2 $[kg/s]$	J_m	1.0 $[kgm^2]$
$-X_{u\|u\|}$	500 $[kgm]$		
m_f	$\gamma\rho Al$ $[kg]$	a	0.25
l	0.30 $[m]$	α_1	-0.9435
D	0.30 $[m]$	α_0	0.4243
A_p	$\frac{\pi}{4}D^2$ $[m^2]$	β_1	-0.1212
ρ	1025 $[kg/m^3]$	β_0	0.0626

Table 1. Model parameters

$T_{\|n\|n}$	3.523
$T^0_{\|n\|u_a}$	-23.74
$Q_{\|n\|n}$	0.1559
$Q^0_{\|n\|u_a}$	-0.9148

Table 2. Thrust and Moment Parameters

Thus,

$$d_{f0} = \frac{-X_u}{(1-t)(1+a)(1-w)} \quad (34)$$

$$d_f = \frac{-X_{u|u|}}{(1-t)(1+a)a(1-w)^2} \quad (35)$$

If these relations between the damping parameters are not satisfied, the steady-state values will not be correct.

7. COMPUTER SIMULATIONS

We are to simulate the dynamic thruster model. The motor is assumed to be a current controlled DC-motor, $Q_m = k_m i_m$ where i_m is the motor current, and k_m its torque coefficient. Assume that the axial flow parameter a, the wake fraction number w, and the thrust deduction number t are constant. The axial flow parameter a is set to $a = 0.25$.

The parameters for the thruster force and hydrodynamic moment mappings are given in Table 2.

Description of the simulated case: At $t = 0$ the vessel is at rest and all states are zero. The following input signal was used

$$k_m i_m = \begin{cases} 5 & 0 \le t \le 0.3t_f \\ -5 & 0.3t_f < t \le 0.6t_f \\ 2.5 & 0.6t_f < t \le t_f \end{cases} \quad (36)$$

Simulation results are shown in Figures 4 and 5. The first shows speed and axial flow and demonstrates the significant difference between the two. Had u_a been used instead of u_p in the propeller equations, dynamic properties would clearly have been wrong.

The thrust and torque shown in Fig. 7 demonstrates, again with the test sequence, verifies that the model operates over a large operational envelope.

The resulting model was used as the basis of a nonlinear observer and controller design for

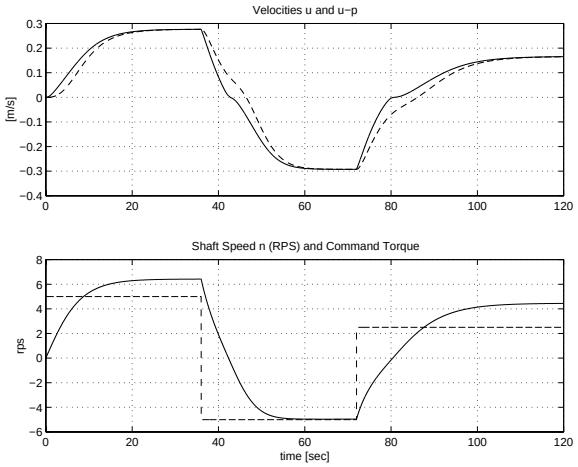

Fig. 4. Axial flow u_p(- -) ship speed u(-) and propeller rotational speed n plotted over time with the test sequence applied. The w and a constants were adjusted to give easy comparison between u and u_p.

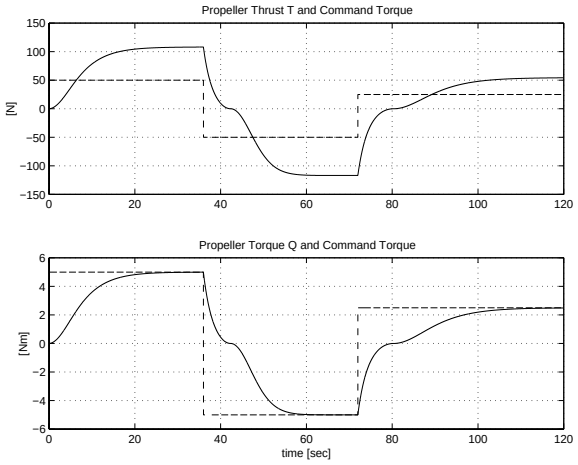

Fig. 5. Propeller thrust and torque over time with the test sequence applied. This verifies the wide envelope operation of the model.

enhanced thruster control (Fossen and Blanke, 2000).

8. CONCLUSIONS

The paper has derived a dynamic model for axial flow and propeller thrust and torque that remedies the shortcoming of an earlier dynamic thruster model, which was valid only around zero forward speed. The model has been simulated and example parameters shown for convenience. The model was formulated using readily available propeller characteristics from open water tests as primary data, showing how these should be modified to obtain the dynamic model.

Real experiments were not available for validation, so simulation was used, showing that the model operates satisfactory also for large manoeuvres with vessel speed ahead or astern.

The dynamics of the tangential flow u_{pt} could play an essential role for the thrust dynamics as well as the axial flow that was the main concern in this paper. The modelling and verification of tangential flow dynamics would hence be a natural extension of the present model.

9. REFERENCES

Blanke, M. (1982). Ship Propulsion Losses Related to Automatic Steering and Prime Mover Control.. PhD thesis. Technical University of Denmark. Lyngby, Denmark.

Breslin, J. P. and P. Andersen (1994). *Hydrodynamics of Ship Propellers*. Cambridge University Press. UK.

Cody, S. E. (1992). An experimental study of the response of small thrusters to step and triangular wave inputs. Technical report. Naval Postgraduate School, Monterey, CA.

Faltinsen, O. M. (1990). *Sea Loads and Offshore Structures*. Cambridge University Press. UK.

Faltinsen, O. M. and B. Sortland (1987). Slow drift eddy making damping of a ship. *Applied Ocean Research* **AOR-9**(1), 37–46.

Fossen, T. I. (1994). *Guidance and Control of Ocean Vehicles*. John Wiley Sons.

Fossen, Thor I. and M. Blanke (2000). Nonlinear output feedback control of underwater vehicle propellers. *IEEE Journal of Oceanic Engineering* **25**(2), 241–255.

Healey, A. J., S. M. Rock, S. Cody, D. Miles and J. P. Brown (1995). Toward an improved understanding of thruster dynamics for underwater vehicles. *IEEE Journal of Oceanic Engineering* **29 (4)**, 354–361.

Lewis, E. W., Ed.) (1988). *Principles of Naval Architecture*. third ed.. Society of Naval Architecture and Marine Engineers. New York.

McLean, M. B. (1991). Dynamic performance of small diameter tunnel thrusters. Technical report. U.S. Naval Postgraduate School, Monterey, CA.

Whitcomb, L. L. and D. Yoerger (1999). Development, comparison, and preliminary experimental validation of nonlinear dynamic thruster models. *IEEE Journal of Oceanic Engineering* **JOE-24**(4), 481–494.

Yoerger, D. R., J. G. Cooke and J.-J. E. Slotine (1991). The influence of thruster dynamics on underwater vehicle behavior and their incorporation into control system design. *IEEE Journal of Oceanic Engineering* **JOE-15**(3), 167–178.